Turning diamond to graphite

Contact s.m.bennington@stfc.ac.uk

S. M. Bennington, T. E. Weller, R. Bewley, K. Ronayne and M. Zhang
Central Laser Facility, STFC, Rutherford Appleton Laboratory, HSIC, Didcot, Oxon OX11 0QX, UK

R. B. Jackmann
London Centre for Nanotechnology, University College London, 17-19 Gordon Street, London, WC1H 0AH, UK

Introduction

Graphene has become one of the most exciting areas of condensed matter physics because of an unusual conflation of interesting fundamental physics and the very real possibility of important technological applications. Not only is it an excellent condensed-matter analogue for two-dimensional quantum electrodynamics [1,2], but it is also a zero band gap semiconductor with room temperature ballistic conduction and electron mobilities at least an order of magnitude greater than in silicon.

Although much of the current interest is focused on graphene it now appears that some of its properties, such as the presence of Dirac Fermions [3,4] and ballistic conduction [5], are also present in graphite [6]. If it becomes possible to make ribbons of graphite with defined edge states (known as zig-zag or arm-chair from the shapes produced when they are cut from a hexagonal graphene sheet) then it may also be possible to control the magnetic properties to make highly magneto-resistive [7] or even half metallic systems [8].

What is hampering both endeavours is a lack of sample; the current method of production is to mechanically cleave graphite. Our aim in this project was to see if it was possible to grow thin layers of graphite through femtosecond laser irradiation of an atomically flat diamond (111) surface. Previous measurements on polycrystalline diamond indicate that it is possible to produce graphite layers several tens of nanometers thick [9], but the thickness and morphology of such surfaces are likely to be governed at least in part by the surface roughness.

During a nanosecond long laser pulse the lattice can attain thermal equilibrium with the excited electrons and the graphitization proceeds through a similar thermal process. However, if the duration of the pulse is reduced to the order of a femtosecond there is no time for the electrons and lattice to come to equilibrium, and a different graphitization mechanism is thought to occur, driven not by the thermal motion of the atoms but by the hot electron-hole plasma [10]. There is evidence for this experimentally; the thickness of a graphite layer produced is controlled primarily by the pulse length [9]; below ~10ps the graphite produced on a polycrystalline diamond surface is a few 10's of nanometers whereas for longer pulses the thickness increases exponentially with pulse length. This is backed by theoretical modelling that shows that thermal graphitization produces inclusions of highly strained graphite that propagate into the bulk [11,12]; whereas a femtosecond pulse will produce a layer by layer reconstruction of the surface of the diamond controlled primarily by the absorption coefficient of the light [9,12].

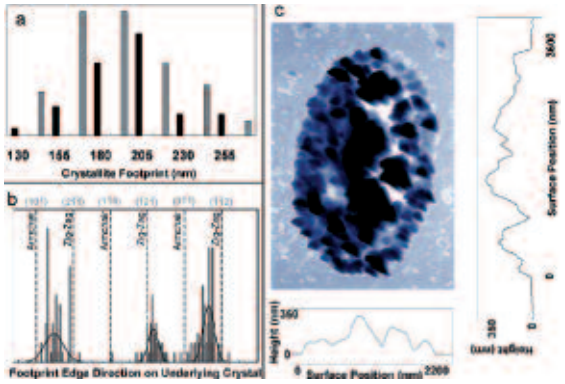

Figure 1. The atomic force microscope (AFM) image of a spot produced with a 120 fs long 800 nm laser pulse with an average fluence of 2 J/cm^2. The spot is made up of a distribution of small triangular graphite crystals. All the crystals have similar orientations within the spot and between different spots and are aligned with respect to the underlying diamond crystal. Insert 1a) shows the orientation of the crystallite footprint edges with respect the diamond crystal. And insert 1b) shows the size distribution of the crystallite footprints.

In this article we describe the morphology of the graphite produced on an atomically flat (111) surface of diamond under femtosecond laser irradiation and speculate about the potential mechanisms for the growth. This is part of a larger piece of work where we are structuring the diamond surface using lithography and Focus Ion Beam milling to produce nanostructures on the diamond prior to graphitization.

Experimental setup

We used a commercial Ti:sapphire laser (provided under the STFC's Laser's for Science programme) to produce pulse widths of 120 fs at a wavelength of 800 nm. By using sum-frequency and 2nd harmonic generation, we also able to produce pulses of 200 nm, 266 nm and 400 nm again with pulse widths of 120 fs.

For the irradiation of the diamond surface a mount specially designed to allow for the short working distances of the objectives was fixed to a piezoelectric positioner. An inverted microscope brought light to focus at the surface, using two different objectives (×10 for 800 nm and Ealing ×74, and all-reflecting for 200 nm, 266 nm, and 400 nm). For the 800 nm experiments, where most of the work was done, the beam profile was asymmetric: approximately Gaussian in one axis with a width measured at 1/e to be 2.2 μm and approximately Lorentzian in the other with a gamma of 6.6 μm.

The diamonds used in this study were single crystal HPHT Type Ib manufactured by Sumitomo, with a pale yellow colour due to ~100 ppm nitrogen concentration. They were cut viscinally at 4° to the (111) crystal and polished so that regions of the diamond were atomically flat as observed in an atomic force microscope (AFM).

Results

At fluences just above the graphitization threshold AFM measurements show an oval spot made up of small triangular features (fig 1). All the triangles have the same orientation implying that they are related to the underlying diamond crystal. There are two distinct ways of cutting a graphene sheet, one produces a zig-zag shaped edge with metallic character and the other has a series of armchair like shapes with a band gap. If the graphene is related to the underlying diamond then the different edges of the triangular features have different edge states: one has a purely zig-zag character and the others two must be mixtures of zig-zag and armchair. The presence of these features was not related to the fluence, but was related to the wavelength; we only observed them when using the 800 nm laser.

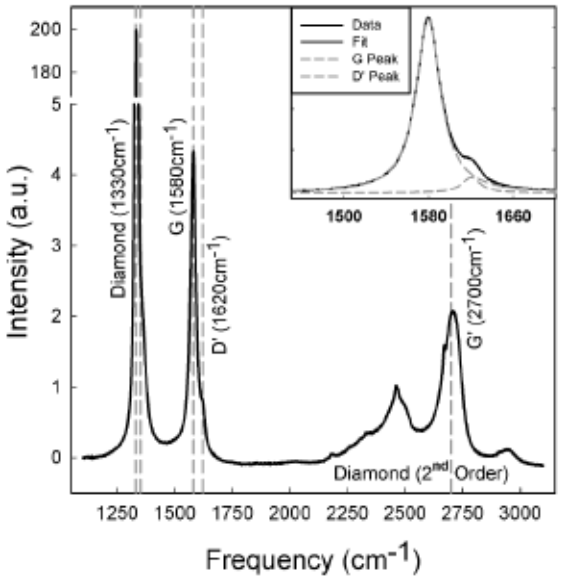

Figure 2. The micro-Raman from a graphite spot produced with 120 fs long 800 nm laser pulse with an average fluence of 2 J/cm^2. It is possible to see a strong diamond peak at 1333 cm^{-1} which masks any defect or D-peak. However, it is possible to see a relatively sharp G-peak with a small D'-peak on one side. The second order G' can be seen around 2700 cm^{-1} within a range of 2nd order diamond excitations. The insert shows a fit to the G and D' peaks.

Micro-Raman (using a wavelength of 514.5 nm) from the centre of these small spots shows a well defined graphite or G-peak centred at 1578.5±0.1 cm^{-1}. The higher harmonic of the defect peak is known to be very sensitive to the graphite stacking[13] and or measurements show a single peak centred at 2706.8±0.2 cm^{-1} with a width of 81.8±0.7 cm^{-1}. The positions and widths of these peaks are consistent with there being disorder in the graphite stacking.

In normal defective graphite it is possible to extract a crystallite size from the ratio of the intensities of the so called defect (D-peak) and graphite (G-peak)[14]. But, the presence of the large diamond peak at 1333 cm^{-1} makes it impossible to see the D-peak clearly at these Raman energies, so we used the ratio of the small D' and G peaks to get an approximate crystallite size of 80 nm. From this it appears that the triangular features observed in the AFM are largely single crystals although without well defined ABAB graphite stacking.

Discussion

There is much speculation that under femtosecond irradiation the transition is not driven thermally but by the dense electron-hole plasma created by the laser[15]. Recent pulsed X-ray diffraction measurements appear to have convincingly proven that this occurs[16,17]. Exciting electrons from the conduction band to the valence band is in effect breaking a bond. Valence force calculations of the change in bonding indicate that the lattice will become unstable once more than ~9% of the electrons are in the conduction band[10]. And measurements of the non-linear optical responses in silicon and GaAs using pump probe techniques, indicate that such high electron-hole densities are indeed achieved for fluencies above the damage threshold[18]. Once excited, the electrons interact strongly, achieving thermal equilibrium in under 10 fs[19], but the interaction with the lattice is much slower and other pump-probe experiments indicate that the electrons persist in their non-equilibrium state for many tens of picoseconds[18,20]. If the DFT calculations are correct then the transformation to graphite will be complete in one or two hundred femtoseconds[12,21], such that the transition to will occur well before the temperature of the lattice rises significantly.

Other density functional calculations have explored the electron lattice interaction in more detail, showing that valence excitons are likely to bind together in high density electron-hole plasmas[22]. A lone valence exciton is not predicted to self trap, but the biexciton is calculated to have a large self trapping lattice distortion that involves the breaking of a bond perpendicular to the (111) direction.

Graphite is a semi-metal and any electron-hole pairs migrating from the diamond to the graphite seed would rapidly multiply in number through impact ionization. Since this would also reduce their average energy below that of the diamond band gap, the electron-hole pairs will be trapped and collect in the

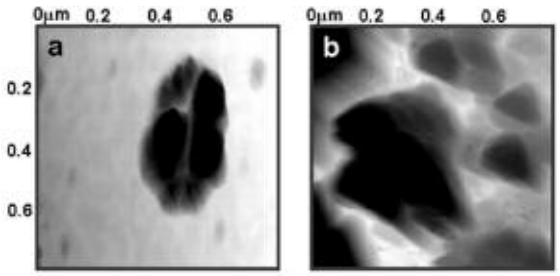

Figure 3. AFM images a) of a spot produced by a 120 fs long 200 nm laser with a total energy of 2 µJ, below the threshold of ablation for this microscope set-up, and b) the graphite crystals produced with 120 fs and 800 nm. There is no evidence for the same crystallite features that we see at 800 nm.

graphite. Graphite is able to support a large number of electron-hole pairs in its π-orbital's without affecting the materials covalent bond network. This and the fact that it is a refractory material will make the graphite more stable than diamond under these conditions.

The type of absorption process is controlled by the energy of the laser, its power and the presence of defects. The direct band gap in diamond is 7.3 eV and the indirect is 5.4 eV corresponding to 170 and 230 nm laser light respectively. By measuring the transmission as a function of fluence at 248 nm Preuss *et al.* were able to demonstrate that the absorption was dominated by two-photon events and a band gap of 7.3 eV [23]. But when using 800 nm light the creation of an electron-hole pair would take a least 4 or 5 photons, the probability of which is very low. If there are defects in the diamond that introduce levels within the band gap then this situation becomes more complex. Our type-Ib diamonds contain substitutional nitrogen producing a donor like centre with thermal ionization energy of 1.7 eV [24] and an optical energy of 2.2 eV [25]. However graphitization requires a free surface and steps in the diamond surface are known to produce levels around 3.45 or 2.32 eV [26], which, given their extended nature would make them very efficient at generating electron-hole pairs through a process of two, 2 or 3-photon events. At 200 and 266 nm nucleation sites are no longer necessary; an electron-hole plasma is created through a two-photon process producing a even graphite sheet wherever the laser fluence rises above the graphitisation threshold (fig 3).

Conclusions

In conclusion we have shown that it is possible to grow graphite epitaxially on the (111) surface of diamond. Using 800 nm lasers the graphite is seeded, probably at defects, to produce small triangular graphite crystals. At shorter wavelengths it is possible to produce more even graphite films.

Acknowledgements

We would like to thank Element-6 for the supply of the diamonds used in this work

References

1. K. S. Novoselov *et al.*, *Nature* **438**, 197 (2005).
2. Y. Zhang *et al.*, *Nature* **438**, 201 (2005).
3. I. A. Luk'yanchuk and Y. Kopeleich, *Phys. Rev. Lett*. **93** (2004).
4. S. Y. Zhou *et al.*, *Nat Phys* **2**, 595 (2006).
5. J. C. Gonzalez *et al.*, *Phys. Rev. Lett*. **99** (2007).
6. Y. Kopelevich and P. Esquinazi, *Adv. Mater*. **19**, 4559 (2007).
7. L. Pisani *et al.*, *Physical Review B* (Condensed Matter and Materials Physics) **75** (2007).
8. Y. W. Son, M. L. Cohen and S. G. Louie, *Nature* **444** (2006).
9. V. V. Kononenko *et al.*, *Quantum electronics* **35**, 252 (2005).
10. P. Stampfli and K. H. Bennermann, *Physical Review B* (Condensed Matter and Materials Physics) **42**, 7163 (1990).
11. G. Kern and J. Hafner, *Phys. Rev. B* **58**, 13167 (1998).
12. C. Z. Wang *et al.*, *Phys. Rev. Lett*. **85**, 4092 (2000).
13. A. C. Ferrari *et al.*, *Phys. Rev. Lett*. **97**, 187401 (2006).
14. L. G. Cancado *et al.*, *Appl. Phys. Lett*. **88**, 163106 (2006).
15. S. K. Sundaram and E. Mazur, *Nature Materials* **1**, 217 (2002).
16. C. W. Siders *et al.*, *Science* **286**, 1340 (1999).
17. A. Rousse *et al.*, *Nature* **410**, 65 (2001).
18. K. Sokolowski-Tinten, J. Bialkowski and D. Von der Linde, *Physical Review B* (Condensed Matter and Materials Physics) **51**, 14186 (1995).
19. T. Elsaesser *et al.*, *Phys. Rev. Lett*. **66**, 1757 (1991).
20. D. H. Reitze, H. Ahn and M. C. Downer, *Physical Review B* (Condensed Matter and Materials Physics) **45**, 2677 (1992).
21. H. O. Jeschke, M. E. Garcia and K. H. Bennemann, *Applied Physics A: Materials Science & Processing* **69**, S49 (1999).
22. F. Mauri and R. Car, *Phys. Rev. Lett*. **75**, 3166 (1995).
23. S. Preuss and M. Stuke, (AIP, 1995), pp. 338.
24. J. Walker, *Rep. Prog. Phys*. **42**, 108 (1979).
25. J. Rosa *et al.*, *Diam. Relat. Mat*. **8**, 721 (1999).
26. B. N. Davidson and W. E. Pickett, *Phys. Rev. B* **49**, 14770 (1994).